Energy-Efficient Joint Handover and Beam Switching Scheme for Multi-LEO Networks

Sz-Han Chen, Li-Hsiang Shen‡, Kai-Ten Feng, Lie-Liang Yang*, and Jen-Ming Wu†
Department of Electronics and Electrical Engineering, National Yang Ming Chiao Tung University, Hsinchu, Taiwan
‡Department of Communication Engineering, National Central University, Taoyuan, Taiwan
*Next Generation Wireless, University of Southampton, Southampton, UK
†Next-generation Communications Research Center, Hon Hai Research Institute, Taipei, Taiwan
Email: henrychen.ee11@nycu.edu.tw, shen@ncu.edu.tw, ktfeng@nycu.edu.tw,
lly@ecs.soton.ac.uk, and jen-ming.wu@foxconn.com

***Abstract*—Low Earth orbit (LEO) has a significant potential to provide ubiquitous global coverage with high capacity data services in sixth generation (6G) wireless networks. Due to the denser deployment of LEO satellites, it becomes mandatory to mitigate the interference induced by LEO beams. The high mobility of LEOs further stirs up a complex interference scenario different from conventional terrestrial networks. Therefore, we conceive a multi-LEO constellation that incorporates multi-beamforming and handover by using only the information of signal-to-interference-plus-noise ratio (SINR) and beam indexes. In this paper, we propose a joint LEO handover and fast beam switching (HOBS) algorithm that performs handover, beam search, and beam/power resource allocation. Our goal is to maximize energy efficiency (EE) while satisfying the SINR requirement of each user. We evaluate our proposed HOBS scheme in terms of different user densities, time frame sizes, and beam-sweeping schemes. Benefiting from a comparatively smaller beam search space, HOBS is capable of providing lower latency, as well as higher SINR and EE compared to conventional exhaustive beam search and fixed power control.**

I. Introduction

Rapid developments in technologies such as the Internet of Things, distributed artificial intelligence, and unmanned vehicles have led to a rapid surge in demand for high-bandwidth transmission. Beyond fifth generation and sixth generation (B5G/6G) communications [1], [2] offer ultra-wide bandwidth and low-latency capabilities that empower high-throughput services. To meet the high demands of B5G/6G and expand network coverage, low Earth orbit (LEO) satellites are becoming the cornerstone to enhance global connectivity. The unique orbital characteristics of LEO satellites grant them various advantages, such as low latency, rapid data transmission, and periodic services over specific regions. To deal with high pathloss compared to terrestrial networks, the beamforming technique is used to concentrate power within a certain area to achieve high beam gain. Furthermore, due to lower deployment costs compared to traditional satellites, some companies, such as SpaceX, Telesat, and Amazon, have launched thousands of LEO satellites [3], aiming to establish seamless coverage.

[1]This work was supported in part by the National Science and Technology Council (NSTC) under Grant 110-2221-E-A49-041-MY3, Grant 112-2218-E-A49-020, Grant 112-2218-EA49-023, Grant 112UC2N006, Grant 112UA10019; in part by STEM Project; in part by the Higher Education Sprout Project of the National Yang Ming Chiao Tung University (NYCU) and Ministry of Education (MoE); in part by the Co-creation Platform of the Industry-Academia Innovation School, NYCU, under the framework of the National Key Fields Industry-University Cooperation and Skilled Personnel Training Act, from the MOE and industry partners in Taiwan, and in part by the Hon Hai Research Institute, Taipei, Taiwan. L.-L. Yang would like to acknowledge the financial support of the Engineering and Physical Sciences Research Council (EPSRC) project EP/X01228X/1.

Various research topics have emerged in the realm of LEO networks, addressing different aspects of their operation. In [4], authors explore the strategy of deactivating unnecessary beams to mitigate inter-beam interference and preserve onboard power. In [5] studies joint optimization of power allocation and beam pattern selection in a single-beam scenario. The work of [6] employs the determinant point process to address the beam hopping (BH) problem in the dual satellite system. In [7], they propose a resource allocation for the BH-based LEO satellite system in the spectrum sharing scenario. Solutions in [5]–[7] necessitate channel state information as input data, which is impractical due to the significant distance between the LEO satellites and the ground users.

Frequency reuse is a common technique in LEO satellite systems due to the scarcity of available bandwidth resources. However, lower frequency reuse numbers will induce higher inter-beam interference. In [8], they used the beam steering technique to alleviate interference between LEO and geostationary orbit (GEO). In [9], they propose a joint multi-beam power control method for the LEOs and GEO to alleviate the co-channel interference. The aforementioned solutions focus mainly on mitigating interference between LEO and GEO satellites, while inter-LEO interference becomes more important in the ultra-dense LEO network [10].

Moreover, handover in LEO satellite systems may occur frequently due to the rapid movement of LEOs, resulting in a more considerable overhead compared to terrestrial networks. There is abundant research on how to design efficient handover strategies. In [11], they propose a handover algorithm that predicts the remaining observable time of the LEO satellites. Although this method reduces the handover rate, it relies on frequent information feedback from the user and LEO locations. The work of [12] adopts user preference to determine the handover process. However, the handover algorithm operates in a centralized manner, requiring the ground gateways to collect additional information. In [13], a user-centric handover scheme is proposed to achieve seamless handovers by buffering downlink data on multiple satellites simultaneously. However, this approach may be infeasible in dense user scenarios, where all satellites require substantial buffering capacity.

None of the existing papers jointly consider beam association and handover overhead for sustaining high energy efficiency of LEO satellites. In this paper, we take into account historical signal-to-interference-plus-noise ratio (SINR) data during the handover decision-making process. We propose a novel beam-training-based handover algorithm to facilitate high-throughput,

979-8-3503-8741-4/24/$31.00 ©2024 IEEE

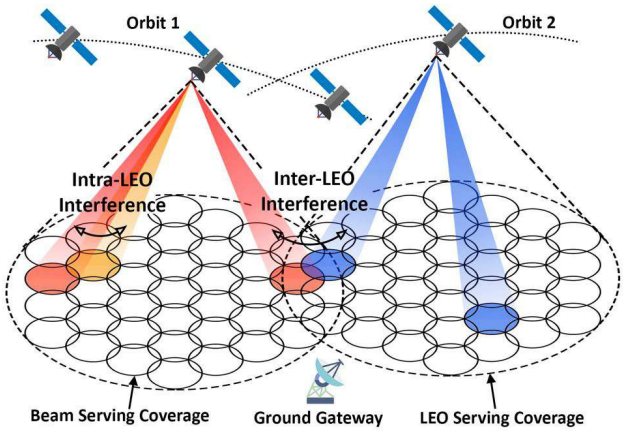

Fig. 1. System architecture of multi-LEO satellite constellations. Several interferences are considered, including inter-beam and inter-LEO interferences.

low power consumption, and low-latency transmission. The key contributions of this paper are summarized as follows:

- We establish a multi-LEO multi-beam constellation following a practical commercial constellation. We consider beamforming overhead and various interference types, including intra-LEO and inter-LEO interferences.
- We propose a joint LEO handover and fast beam switching (HOBS) algorithm which iteratively allocates beam and power resources, as well as performs handover for users experiencing poor signal quality. Note that HOBS relies solely on SINR feedback to determine its actions.
- In simulations, we evaluate HOBS in terms of different user densities, time frame sizes, and beam sweeping schemes. Benefited by comparably smaller beam searching space, HOBS is capable of providing lower latency and higher SINR and energy efficiency (EE) compared to conventional exhaustive beam search (EBS).

The rest of this paper is organized as follows. Section II describes the LEO system model. In Section III, we define the EE optimization problem. Section IV elaborates on the proposed HOBS scheme. Section V provides the simulation results, whilst the conclusions are drawn in Section VI.

II. System Model

As shown in Fig. 1, we consider a multi-LEO satellite communication system consisting of N LEOs indexed by $n \in \mathcal{N} \triangleq \{1, ..., N\}$, serving a total of K randomly distributed ground users indexed by $k \in \mathcal{K} \triangleq \{1, ..., K\}$. Each LEO has equivalent M beam cells, where each cell is indexed by $m \in \mathcal{M} \triangleq \{1, ..., M\}$. Note that the ground gateway is deployed to associate LEOs for initial control signaling.

A. Signal Model

In the LEO satellite systems, signal fading is a crucial factor due to the long distance of signal propagation. Unlike terrestrial networks, attenuation caused by tropospheric effects must be considered [14]. The total path loss in units of dB can be expressed as

$$L = L_{fs} + L_g + L_{sc} + L_{sf}, \tag{1}$$

where free space path loss L_{fs} is given by

$$L_{fs} = 20\log(f_c) + 20\log(d) - 147.55, \tag{2}$$

with f_c as the central operating frequency and d as the distance between the LEO and ground user. L_g is atmospheric absorption loss, with various types of gases and particles that absorb the electromagnetic wave of specific frequencies. L_{sc} denotes the tropospheric scintillation effect caused by the rapid variation in the refractive atmosphere. Shadow fading L_{sf}, caused by blockage in the line-of-sight (LOS) propagation path, follows a log-normal distribution. The pertinent expressions and lookup table of these factors can be found in [14], [15].

We adopt the antenna radiation pattern in [16] for the LEO satellites denoted as

$$G(\theta) = G_0 \left[\frac{J_1(\mu(\theta))}{2\mu(\theta)} + 36\frac{J_3(\mu(\theta))}{\mu(\theta)^3} \right]^2, \tag{3}$$

where θ is the boresight angle, and G_0 is the maximum antenna gain defined as $G_0 = \eta\frac{4\pi A}{(c/f_c)^2}$, where η is the antenna efficiency, A is the antenna aperture size, c is the velocity of the light. $J_1(\cdot)$ and $J_3(\cdot)$ respectively represent the Bessel functions of the first kind of orders 1 and 3, and $\mu(\theta) = 2.07123 \cdot \sin(\theta)/\sin(\theta_{3dB})$, where θ_{3dB} is the 3 dB half-power beamwidth angle of the antenna.

We define the channel gain from the m-th beam of the n-th LEO to the k-th user as $H_{n,m,k} = 10^{-L/10}$. Therefore, the SINR of the ground user k served by the beam m of LEO n can be formulated as

$$\gamma_{n,m,k}(t) = \frac{P_{n,m}(t)H_{n,m,k}(t)G^T_{n,m,k}(t)G^R_{n,m,k}(t)a_{n,m,k}(t)}{I^a_{n,m,k} + I^b_{n,m,k} + \sigma^2}, \tag{4}$$

where $P_{n,m}(t)$ is the transmit power of beam m at satellite n, $G^T_{n,m,k}(t)$ and $G^R_{n,m,k}(t)$ are the transmitting and the receiving antenna gain, respectively, and σ^2 is the power of the thermal noise. The association indicator $a_{n,m,k} = 1$ when user k is served by the beam m of satellite n; otherwise, $a_{n,m,k} = 0$. We further define the exclusive set of $\mathcal{N}' \triangleq \mathcal{N}\backslash n$, $\mathcal{M}' \triangleq \mathcal{M}\backslash m$ and $\mathcal{K}' \triangleq \mathcal{K}\backslash k$. Intra-LEO interference $I^a_{n,m,k}$ in (4) is

$$I^a_{n,m,k} = \sum_{m' \in \mathcal{M}'} \sum_{k' \in \mathcal{K}'} P_{n,m'}(t)H_{n,m',k}(t) \cdot G^T_{n,m',k}(t)G^R_{n,m',k}(t)a_{n,m',k'}(t). \tag{5}$$

Similarly, inter-LEO interference $I^b_{n,m,k}$ can be expressed as

$$I^b_{n,m,k} = \sum_{n' \in \mathcal{N}'} \sum_{m' \in \mathcal{M}} \sum_{k' \in \mathcal{K}'} P_{n',m'}(t)H_{n',m',k}(t) \cdot G^T_{n',m',k}(t)G^R_{n',m',k}(t)a_{n',m',k'}(t). \tag{6}$$

B. Beam Training Process

As shown in Fig. 2, the LEO satellites execute beam training [17], [18] in each data frame to align the best beam to achieve modest signal quality. At the start of one transmission frame, the LEO will send the beacon message from each beam to the ground users. The ground users will then send the feedback information back to the satellites, including the optimal beam index and its corresponding SINR. We can observe that a longer beam alignment time will reduce the data transmission time.

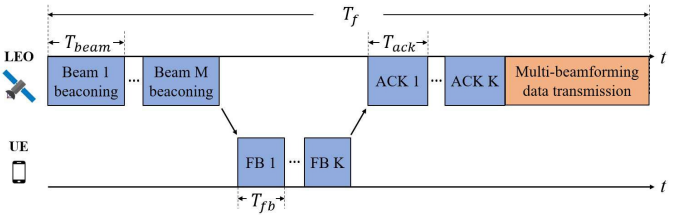

Fig. 2. The beam training process in one transmission frame.

Therefore, it is important to minimize the training time while guaranteeing a high SINR for each user. The training latency of an LEO in a single transmission frame can be expressed as

$$C_n(t) = |\phi_n^{LEO}(t)| \cdot T_{beam} + \sum_{m \in \mathcal{M}} U_{n,m}(t) \cdot (T_{fb} + T_{ack}), \tag{7}$$

where T_{beam} is the time duration of one beam beaconing. $U_{n,m}(t)$ is the number of users served by the m-th beam of the n-th satellite. T_{fb} and T_{ack} denote the feedback and acknowledgment intervals, respectively. $\phi_n^{LEO}(t)$ is the beam training set containing the beams that need to be scanned by the n-th satellite, which can be expressed as

$$\phi_n^{LEO}(t) = \{(n,m) \in \mathbf{\Phi}(t) \mid \forall m \in \mathcal{M}\}, \tag{8}$$

where $\mathbf{\Phi}(t)$ is the beam training set of the LEO constellation. The detailed definition of $\mathbf{\Phi}(t)$ will be elaborated in Section IV.

Therefore, the latency-aware throughput of the k-th user which is served by the m-th beam of the n-th satellite is given by

$$R_{n,m,k}(t) = \left(1 - \frac{C_n(t)}{T_f}\right) \frac{W_{n,m}}{U_{n,m}(t)} \log_2\left(1 + \gamma_{n,m,k}(t)\right), \tag{9}$$

where T_f is the time interval of the entire transmission frame and $W_{n,m}$ is the bandwidth of the m-th beam in n-th LEO. We allocate the bandwidth equally among the users served by the same beam to ensure fairness. Furthermore, we define a successful beam training if the optimal beam SINR is greater than a threshold γ_{thr}, namely $\gamma_{n,m,k} \geq \gamma_{thr}$. A weak beam with a low SINR will result in failure of beam training. We define beam alignment accuracy as

$$Q_{n,m,k}(t) = \frac{1}{S} \sum_{\tau=t-S+1}^{t} \mathbb{1}(\gamma_{n,m,k}(\tau) \geq \gamma_{thr}), \tag{10}$$

where S is the historical observable window size and the value of the indicator function $\mathbb{1}(\cdot)$ is one if the statement is true.

The achievable sum-rate of all users under the LEO satellite constellation is denoted as

$$R_{tot}(t) = \sum_{n \in \mathcal{N}} \sum_{m \in \mathcal{M}} \sum_{k \in \mathcal{K}} R_{n,m,k}(t), \tag{11}$$

and the total beam alignment accuracy is expressed as

$$Q_{tot}(t) = \sum_{n \in \mathcal{N}} \sum_{m \in \mathcal{M}} \sum_{k \in \mathcal{K}} Q_{n,m,k}(t). \tag{12}$$

Since LEO satellites rely on solar power, optimizing EE becomes a crucial aspect of the resource allocation problem in LEO networks. The EE performance of beam m of LEO n at time t is expressed as

$$E_{eff}(t) = \frac{R_{tot}(t)}{\sum_{n \in \mathcal{N}} \sum_{m \in \mathcal{M}} P_{n,m}(t)}. \tag{13}$$

III. Problem Formulation

As mentioned above, it becomes compellingly imperative to achieve maximum EE by allocating power, association indicator, and candidate beam training set. We define the solutions of power $\boldsymbol{P} = \{P_{n,m}(t) \mid \forall n \in \mathcal{N}, \forall m \in \mathcal{M}\}$, association indicator $\boldsymbol{a} = \{a_{n,m,k}(t) \in \{0,1\} \mid \forall n \in \mathcal{N}, \forall m \in \mathcal{M}, \forall k \in \mathcal{K}\}$ and beam training set $\mathbf{\Phi} = \left\{(n,m) \mid \forall n \in \mathcal{N}, m \in \phi_n^{LEO}(t)\right\}$ containing the pairs of beam index m of LEO n. To maximize energy efficiency, our objective is for the satellites to allocate power to each beam in a way that balances high data rates with low interference. Accordingly, the optimization problem can be formulated as

$$\max_{\boldsymbol{P},\boldsymbol{a},\mathbf{\Phi}} \quad E_{eff}(t) \tag{14a}$$

$$\text{s.t.} \quad R_{n,m,k}(t) \geq R_{th}, \quad \forall n \in \mathcal{N}, \forall m \in \mathcal{M}, \forall k \in \mathcal{K}, \tag{14b}$$

$$Q_{n,m,k}(t) \geq \delta, \quad \forall n \in \mathcal{N}, \forall m \in \mathcal{M}, \forall k \in \mathcal{K}, \tag{14c}$$

$$Q_{tot}(t) \geq \delta_t, \tag{14d}$$

$$C_n(t) \leq \rho, \quad \forall n \in \mathcal{N}, \tag{14e}$$

$$\sum_{n \in \mathcal{N}} C_n(t) \leq \rho_t, \tag{14f}$$

$$0 \leq P_{n,m}(t) \leq P_{beam}, \quad \forall n \in \mathcal{N}, \forall m \in \mathcal{M}, \tag{14g}$$

$$0 \leq \sum_{m \in \mathcal{M}} P_{n,m}(t) \leq P_{max}, \quad \forall n \in \mathcal{N}. \tag{14h}$$

Constraint (14b) guarantees the throughput of each user k to be above the threshold R_{th}. Constraint (14c) guarantees the individual beam alignment accuracy δ. Constraint (14d) restricts the total system beam training accuracy to surpass the threshold as δ_t. Constraint (14e) ensures that the training time per beam is limited to be shorter than ρ. Constraint (14f) restricts the overall beam training latency to be within the specified threshold ρ_t. Constraint (14g) denotes the maximum beam power P_{beam} allowed for each beam. Constraint (14h) restricts the total transmit power of each LEO to be less than P_{max}. Due to the presence of mixed continuous and discrete variables in the optimization problem, it becomes intractable and cannot be solved directly by conventional optimization.

IV. Proposed HOBS Algorithm

The conventional beam training scheme involves sweeping through all beam sectors to obtain the globally optimal SINR. However, this training process introduces an unaffordable overhead, which leads to little time for data transmission. To address this, we propose to utilize the historical SINR for beam training in order to reduce beam training overhead. Note that the total data rate R_{tot} can be acquired at the ground gateway by aggregating information from LEOs. Consequently, the LEO satellites collaboratively allocate their beam and power resources to mitigate interference. Therefore, the original optimization problem in (14) can be separated into two subproblems, i.e., beam training association and power allocation.

To deal with these two sub-problems, we propose an LEO handover and fast beam switching algorithm as well as a power control mechanism, which are introduced in the following subsections.

A. Joint LEO Handover and Fast Beam Switching

The first sub-problem regarding user association and beam training can be expressed as

$$\max_{\boldsymbol{a},\boldsymbol{\Phi}} \quad R_{tot}(t) \tag{15a}$$

$$\text{s.t.} \quad (14b), (14c), (14d), (14e), (14f). \tag{15b}$$

The proposed beam training is summarized in Algorithm 1, whereas the handover decision process is demonstrated in Algorithm 2. The algorithms aim to maximize signal quality while minimizing beam training time. Let us elaborate on the details of Algorithm 1. Initially, the satellites sweep all beam cells when there is no historical data available. After the historical observable time window size S, the algorithm selects the most recent successful LEO beam pair by (n, m), with its SINR $\gamma_{n,m,k}$ greater than the threshold γ_{thr}. We define $\phi^S_{best}(t) = \{\phi_{best}(t-s) \mid \forall s \in \{1, 2, ..., S\}\}$ as the best serving beams within the time window S. The functions $\mathrm{x}(\cdot)$ and $\mathrm{y}(\cdot)$ attain the practical coordinates of the beam indices on the horizontal and vertical axes, respectively. The function $\mathrm{diff}(\cdot)$ calculates the differences in the beam indexes between two consecutive time frames, i.e., $\mathrm{diff}(\boldsymbol{x}) = \{x_{t+1} - x_t \mid t \in \{1, ..., S-1\}\}$, where $\boldsymbol{x} = [x_1, ..., x_S]$. We define the coordinate difference array as

$$L^z_{best}(t) = \ \mathrm{diff}(\mathrm{z}(\phi^S_{best}(t))), \ \forall \mathrm{z} \in \{\mathrm{x}, \mathrm{y}\}. \tag{16}$$

For example, if the coordinates of the best beams in the time window $S = 4$ are expressed as $\mathrm{x}(\phi^S_{best}(t)) = [10, 20, 5, 10]$, $L^x_{best}(t) = [10, -15, 5]$. The beam search ranges of ε_x and ε_y are determined by multiplying the number of consecutive failures, which can be given by

$$\varepsilon_z = s \cdot \max|L^z_{best}(t)|, \ \forall z \in \{x, y\}. \tag{17}$$

The adaptive strategy addresses the uncertainty of the optimal beam location. If there is no failure beam within the historical window size S, i.e., the values are all positive or negative, a smaller size of beam training will be performed; otherwise, the larger beam training size will be carried out. The beam training set is expressed as

$$\phi^z_k(t) = \begin{cases} \{\psi \in \boldsymbol{\Psi} \mid \mathrm{z}(\psi) \in [\mathrm{z}(n,m), \ \mathrm{z}(n,m) + \varepsilon_z]\}, \\ \qquad\qquad \text{if } \min L^z_{best}(t) \geq 0, \\ \{\psi \in \boldsymbol{\Psi} \mid \mathrm{z}(\psi) \in [\mathrm{z}(n,m) - \varepsilon_z, \ \mathrm{z}(n,m)]\}, \\ \qquad\qquad \text{if } \max L^z_{best}(t) \leq 0. \\ \{\psi \in \boldsymbol{\Psi} \mid \mathrm{z}(\psi) \in [\mathrm{z}(n,m) - \varepsilon_z, \ \mathrm{z}(n,m) + \varepsilon_z]\}, \\ \qquad\qquad \text{otherwise}, \end{cases} \tag{18}$$

where $\boldsymbol{\Psi} = \{(n, m) \mid \forall n \in \mathcal{N}, \forall m \in \mathcal{M}\}$ contains all beams formed by the LEO network. The beam training set consists of the beams that are in both $\phi^x_k(t)$ and $\phi^y_k(t)$. The training beam set contributed by user k is expressed as

$$\phi_k(t) = \phi^x_k(t) \cap \phi^y_k(t), \tag{19}$$

Algorithm 1: Proposed HOBS Algorithm

Initialization:
Set the best historical beam set with window size S as ϕ^S_{best}
while LEO constellation is operating **do**
  $t = t + 1$
  for $k \in \mathcal{K}$ **do**
    if $t < S$ **or** $Q_{n,m,k}(t) < \delta$ **then**
      $\phi_k(t) = \mathcal{M}$
      continue
    end if
    for $s \in \{1, ..., S\}$ **do**
      if $\phi^S_{best}(t-s) \geq \gamma_{thr}$ **then**
        $(n, m) = \phi^S_{best}(t-s)$
        break
      end if
    end for
    $L^z_{best}(t) = \mathrm{diff}(\mathrm{z}(\phi^S_{best})), \quad \forall \mathrm{z} \in \{\mathrm{x}, \mathrm{y}\}$
    $\varepsilon_z = s \cdot \max|L^z_{best}(t)|, \quad \forall z \in \{x, y\}$
    Acquire $\phi^z_k(t)$ according to (18), $\quad \forall z \in \{x, y\}$
    $\phi_k(t) = \phi^x_k(t) \cap \phi^y_k(t)$
  end for
  $\boldsymbol{\Phi}(t) = \bigcup_{k \in \mathcal{K}} \phi_k(t)$
end while

where $\cap$ is denoted as the intersection operation. The total beam training set is then expressed as

$$\boldsymbol{\Phi}(t) = \bigcup_{k \in \mathcal{K}} \phi_k(t), \tag{20}$$

where $\bigcup$ is the union operation.

Once the beam candidates are established at each LEO, the beams are trained to obtain SINR feedback from the ground users for the next prediction. In the following, we propose three beam training mechanisms.

1) Synchronous Consecutive Beam Sweeping (SCBS): As shown in Fig. 3(a), complete synchronization is considered among all LEO satellites, ensuring that the beam training for an LEO is not affected by other satellites. Although this mechanism can obtain the best beams without interference, it results in substantial training overhead due to consecutive training. The total beam training overhead can be formulated as

$$T_{SCBS} = \sum_{n \in \mathcal{N}} C_n(t). \tag{21}$$

2) Synchronous Simultaneous Beam Sweeping (SSBS): As shown in Fig. 3(b), all LEO satellites are synchronized by executing beam training concurrently. This approach significantly reduces the overall training latency compared to SCBS. However, it induces inter-beam interference during the training phase. Therefore, the user feedback may be inaccurate due to interference from other satellites. The total training latency is given by

$$T_{SSBS} = \max_n C_n(t). \tag{22}$$

3) Asynchronous Beam Sweeping (ABS): As shown in Fig. 3(c), this scheme operates under the consideration that LEO satellites are not synchronized. They perform beam training when other satellites conduct data transmission. Unlike SSBS, all satellites will conduct their data transmission right after the

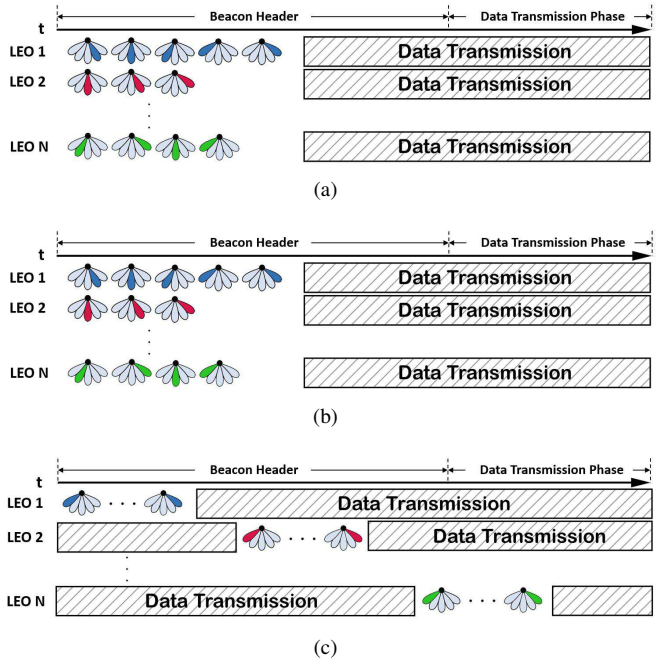

Fig. 3. Proposed beam sweeping schemes: (a) SCBS (b) SSBS (c) ABS.

completion of beam training. The average training latency is expressed by

$$T_{ABS} = \mathbb{E}\left[C_n\right] = \frac{1}{N}\sum_{n\in\mathcal{N}} C_n(t), \tag{23}$$

where $\mathbb{E}\left[C_n\right]$ is the expected latency over all LEOs.

Once all candidate beams have been scanned, the necessity of handover will be determined. To achieve the highest throughput, the beams available with the highest SINR are selected for each user. Moreover, to avoid ping-pong effects in inter-LEO handover, two criteria are employed. The first criterion ensures that the beam SINR of the target LEO exceeds that of the original cell with a specified offset γ_{os}, which is expressed as

$$\gamma_{n^*,m^*,k}(t) - \gamma_{os} > \gamma_{n,m,k}(t), \tag{24}$$

where $\gamma_{n^*,m^*,k}(t)$ is the SINR of target beam. The second criterion is that the duration for SINR of the target beam cell must exceed the trigger time T_{thr}, which is expressed as

$$T^{trig}_{n^*,m^*,k} \geq T_{thr}, \tag{25}$$

where $T^{trig}_{n^*,m^*,k}$ is the handover trigger time of target beam m^* in LEO n^*, i.e., the duration of satisfaction of (24). An inter-LEO handover process occurs when both conditions are satisfied. The entire handover process is demonstrated in Algorithm 2.

B. Dynamic Power Control (DPC)

To this end, we have solved the beam training and handover problem in (15). We can proceed to reckon with power allocation associated with the second sub-problem given by

$$\max_{\boldsymbol{P}} \quad E_{eff}(t) \tag{26a}$$

$$\text{s.t.} \quad (14g), (14h). \tag{26b}$$

Algorithm 2: Handover Process in HOBS

Initialization:
Set trigger time threshold of inter-LEO handover T_{thr}, the decision offset of inter-LEO handover γ_{os}, and the current trigger time $T^{trig} = \{T^{trig}_{n,m,k} \mid \forall n \in \mathcal{N}, \forall m \in \mathcal{M}, \forall k \in \mathcal{K}\}$.
Sort $\phi_k(t)$ according to the SINR of each beam in descending order.
for $(n^*, m^*) \in \phi_k(t)$ **do**
  if $n = n^*$ **then**
    if $\gamma_{n^*,m^*,k}(t) > \gamma_{n,m,k}$ **then**
      Intra-LEO handover from beam m to m^*
      break
    end if
  else
    if condition (24) and (25) are satisfied **then**
      Inter-LEO handover to beam m^* in LEO n^*
      break
    end if
  end if
  Update the $T^{trig}_{n,m,k}$ based on the $\gamma_{n^*,m^*,k}(t)$
end for

We can observe that the EE maximization involves the temporal decision for all beams, which cannot be readily solved by convex optimization methods. Therefore, we propose a low complexity power control for adjusting the power of each beam which is expressed as

$$P_{n,m}(t) = P_{n,m}(t - T_f) + \xi^P_{n,m}(t). \tag{27}$$

The power control coefficient $\xi^P_{n,m}(t)$ varies based on the observation of the objective EE $E_{eff}(t)$, which is designed as

$$\xi^P_{n,m}(t) = \begin{cases} -\xi^P_{n,m}(t - T_f), & \text{if } E^{eff}_{n,m}(t) \leq E^{eff}_{n,m}(t - T_f), \\ \xi^P_{n,m}(t - T_f), & \text{otherwise}, \end{cases} \tag{28}$$

where the individual EE of beam m in LEO n is denoted as

$$E^{eff}_{n,m}(t) = \frac{\sum_{k\in\mathcal{K}} R_{n,m,k}(t)}{P_{n,m}(t)}. \tag{29}$$

If a lower per-beam EE is obtained, it will adjust the beam power to achieve a higher EE. Note that improving individual EE can guarantee the total EE enhancement in $E_{eff}(t)$. This approach allows each beam to continuously search for its optimal power in response to dynamic changes of satellite orbits, wireless channel, and interference conditions. To guarantee the SINR of each user, the regulation of $\xi^P_{n,m}(t)$ is expressed as

$$\xi^P_{n,m}(t) = \begin{cases} |\xi^P_{n,m}(t)|, & \text{if } \exists k \in \mathcal{K} : \gamma_{n,m,k} < \gamma_{thr}, \\ \xi^P_{n,m}(t), & \text{otherwise}. \end{cases} \tag{30}$$

This approach avoids the situation in which there is insufficient beam power to provide acceptable service quality. Furthermore, we will adjust the beam power to satisfy the power constraint of (14h), which is given by

$$P_{n,m}(t) = \begin{cases} P_{n,m}(t)\frac{P_{max}}{\sum_{m'\in\mathcal{M}} P_{n,m'}(t)}, & \text{if } \sum_{m'\in\mathcal{M}} P_{n,m'}(t) > P_{max}, \\ 0, & \text{if } P_{n,m}(t) < 0, \\ P_{n,m}(t), & \text{otherwise}. \end{cases} \tag{31}$$

TABLE I
PARAMETERS SETTING

System Parameter	Value
Number of LEOs	165
Number of LEO beams M	37
LEO altitude	550 km
LEO serving radius	500 km
Operating band f_c	28 GHz (Ka-band)
System bandwidth	100 MHz
LEO maximum transmit power P_{max}	50 dBm
Noise power spectral density N_0	-174 dBm/Hz
Antenna aperture	$10c/f_c$ rad
Maximum antenna gain G_0	40 dBi
3dB beamwidth θ_{3dB}	0.058 rad
SINR threshold γ_{thr}	10 dB
Observation window size S	4
Beam accuracy threshold δ	0.7
handover decision offset γ_{os}	6 dB
Beam training duration T_{beam}	500 μs
Feedback duration T_{fb}	50 μs
Acknowledgement duration T_{ack}	50 μs

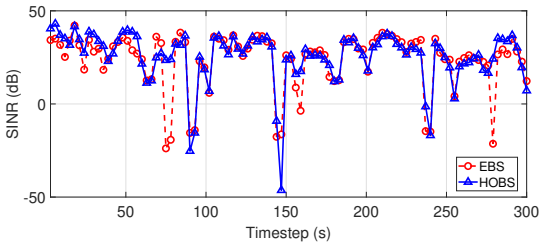

Fig. 4. SINR values of EBS and proposed HOBS algorithm in terms of timestep.

If the beam power exceeds the maximum value of P_{beam}, a normalization process similar to (31) will be performed to satisfy (14g).

V. PERFORMANCE EVALUATION

In this section, we evaluate the performance of the proposed HOBS algorithm in the multi-beam and multi-LEO scenario. The simulation parameters are listed in Table I [3], [19]. Users are randomly and uniformly distributed within the service coverage of all LEOs. The orbit and movement parameters of the LEO follow [20], and the LEO channel-related parameters can be found in [14], [15]. Note that HOBS adopts the ABS scheme in the evaluation of Figs. 4 to 6. As shown in Fig. 4, the SINR of a user is observed by adopting the baseline scheme EBS and the proposed HOBS. EBS always scans all beams to guarantee optimal SINR, but induces unaffordable training overhead. We can see that the proposed HOBS scheme achieves asymptotic SINR to that of EBS while minimizing latency, which can be found in the following discussion.

In Fig. 5, we evaluate HOBS in terms of average throughput and average beam training delay with different user densities $\lambda \in \{2\times10^{-5}, 5\times10^{-5}\}$ users/km^2. HOBS-P indicates HOBS with the proposed DPC, while EBS and HOBS-F adopt full power control (FPC). In Fig. 5(a), it can be seen that HOBS-F and HOBS-P achieve approximately 1.2 times to twice higher throughput compared to EBS. With an increase in the time frame size T_f, the throughput increases due to the lower proportion of the beam training overhead. Furthermore, each user can be allocated more resources with a low user

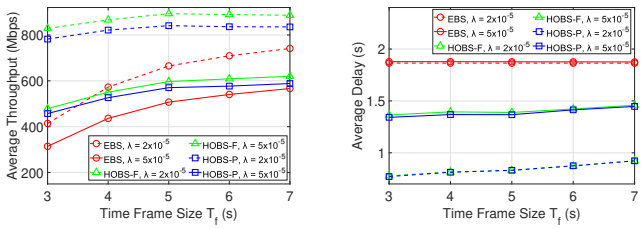

(a) (b)

Fig. 5. (a) average user throughput and (b) average delay of proposed HOBS with DPC under different user densities λ and time interval of transmission frame T_f.

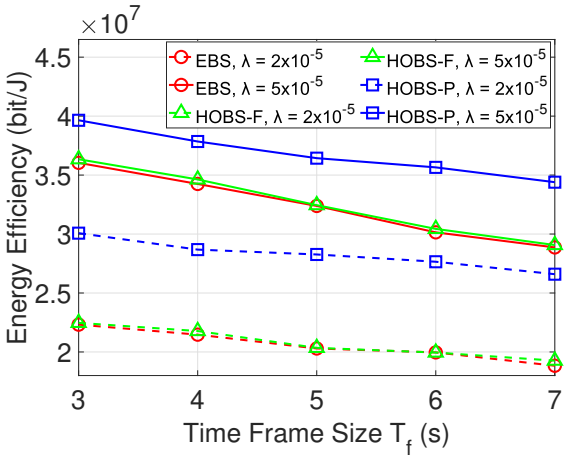

Fig. 6. Energy efficiency of proposed HOBS with baseline EBS in terms of user density λ and time frame size T_f.

TABLE II
AVERAGE BEAM ALIGNMENT ACCURACY

T_f	SCBS	SCBS-P	SSBS	SSBS-P	ABS	ABS-P
2 s	0.895	**0.905**	0.837	0.852	**0.921**	**0.930**
3 s	0.886	0.894	0.829	0.839	**0.911**	**0.918**
4 s	0.874	0.883	0.814	0.823	**0.900**	**0.904**
5 s	0.869	0.876	0.807	0.815	0.894	0.898
6 s	0.846	0.848	0.785	0.789	0.867	0.870
7 s	0.834	0.834	0.774	0.776	0.855	0.856

density, resulting in high user throughput. In Fig. 5(b), HOBS significantly reduces the delay in beam training. However, a higher beam training time is required in a higher user density scenario due to insufficient beam resources and high interference.

In Fig. 6, we can see that HOBS-P can achieve the highest system EE compared to HOBS-F and EBS. With increasing time frame size, the EE decreases due to infrequent power adjustment. This means that beam training cannot be well aligned with power control in a timely manner to address channel variations resulting from the rapid movement of LEOs. Furthermore, historical data will become obsolete more quickly compared to data collected over a shorter time interval, inducing inaccurate beam training. Some users may suffer from low signal quality due to beam misalignment in larger time frame

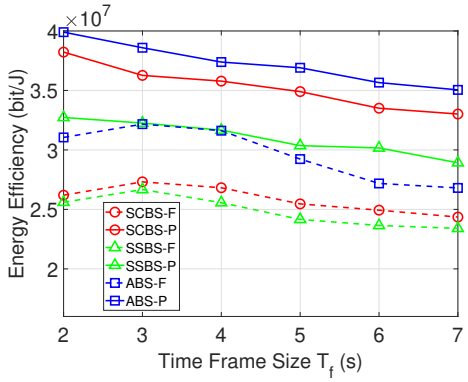

(a)

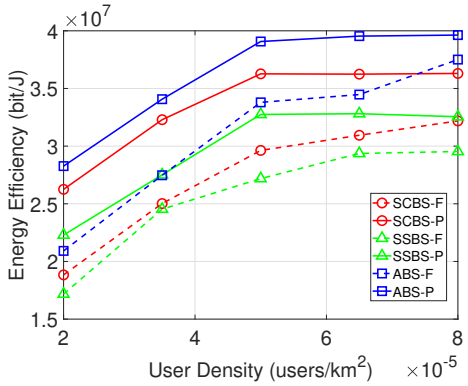

(b)

Fig. 7. Performance of proposed beam sweeping schemes with power control algorithm in terms of the (a) time frame size and the (b) user density.

size, causing all schemes to possess lower EE. As shown in Table II, we list the beam training accuracy of three beam sweeping mechanisms. We can observe that higher beam alignment accuracy is associated with shorter time frame size. Moreover, it can be inferred that ABS achieves the highest beam alignment accuracy, as LEO can immediately perform beam search with continuously updated information.

In Fig. 7(a), we evaluate the performance of different beam sweeping schemes with user density $\lambda = 4 \times 10^{-5}$users/km^2. We can see that the performances of FPC with all the sweeping schemes perform concave shapes of curves. With increasing time frame size $T_f \leq 3$, more data transmission time can be executed to compromise the interference of FPC. However, time frame sizes larger than $T_f \geq 3$ suffer from outdated beam information and high interference. Additionally, the ABS has the highest EE due to its low training latency and high beam alignment accuracy. Although SSBS has generically lower training latency compared to the SCBS, the performance of simultaneous beam sweeping in SSBS will be deteriorated owing to the inter-beam interference, especially in the ultra-dense LEO scenario. In Fig. 7(b), we evaluate the system EE with the time frame size $T_f = 3$. With the increase in user density, it accomplishes higher EE due to the higher probability of better beam search information feedback as well as greater degree of freedom of power allocation. However, the EE performance gradually saturates owing to increasingly insufficient beam and power resources.

VI. Conclusion

In this paper, we have conceived a multi-LEO constellation that integrates multi-beamforming, intra-LEO, and inter-LEO beam handover, solely based on SINR and beam index information. The HOBS scheme is proposed to deal with joint beam search, handover, as well as power control benefited from utilizing historical beam information. The three beam sweeping mechanisms including SSBS, SCBS, and ABS are designed under different scenarios. Simulations have demonstrated the benefits of the proposed HOBS under different beam training schemes in terms of different time frame sizes and user densities. The HOBS with dynamic power control scheme can achieve the highest EE and beam alignment accuracy as well as low latency compared to the conventional EBS.

References

[1] N. Yang and A. Shafie, "Terahertz Communications for Massive Connectivity and Security in 6G and Beyond Era," *IEEE Communications Magazine*, pp. 1–7, 2022.

[2] L.-H. Shen, K.-T. Feng, and L. Hanzo, "Five Facets of 6G: Research Challenges and Opportunities," *ACM Computing Surveys*, vol. 55, no. 11, 2023.

[3] N. Pachler, I. del Portillo, E. F. Crawley, and B. G. Cameron, "An Updated Comparison of Four Low Earth Orbit Satellite Constellation Systems to Provide Global Broadband," in *Proc. IEEE International Conference on Communications Workshops (ICC Workshops)*, 2021, pp. 1–7.

[4] S. Liu, J. Lin, L. Xu, X. Gao, L. Liu, and L. Jiang, "A Dynamic Beam Shut Off Algorithm for LEO Multibeam Satellite Constellation Network," *IEEE Wireless Communications Letters*, vol. 9, no. 10, pp. 1730–1733, 2020.

[5] A. Wang, L. Lei, X. Hu, E. Lagunas, A. I. Pérez-Neira, and S. Chatzinotas, "Adaptive Beam Pattern Selection and Resource Allocation for NOMA-Based LEO Satellite Systems," in *Proc. IEEE Global Communications Conference*, 2022, pp. 674–679.

[6] W. Li, M. Zeng, X. Wang, and Z. Fei, "Dynamic Beam Hopping of Double LEO Multi-beam Satellite based on Determinant Point Process," in *Proc. IEEE International Conference on Wireless Communications and Signal Processing (WCSP)*, 2022, pp. 713–718.

[7] M. Zhang, X. Yang, and Z. Bu, "Resource Allocation with Interference Avoidance in Beam-Hopping Based LEO Satellite Systems," in *Proc. IEEE Information Communication Technologies Conference (ICTC)*, 2023, pp. 83–88.

[8] A. Hills, J. M. Peha, and J. Munk, "Feasibility of Using Beam Steering to Mitigate Ku-Band LEO-to-GEO Interference," *IEEE Access*, vol. 10, pp. 74 023–74 032, 2022.

[9] M. Jia, Z. Li, X. Gu, and Q. Guo, "Joint Multi-beam Power Control for LEO and GEO Spectrum-sharing Networks," in *Proc. IEEE International Conference on Communications in China (ICCC)*, 2021, pp. 841–846.

[10] B. Di, L. Song, Y. Li, and H. V. Poor, "Ultra-Dense LEO: Integration of Satellite Access Networks into 5G and Beyond," *IEEE Wireless Communications*, vol. 26, no. 2, pp. 62–69, 2019.

[11] L. Shi, F. Yang, W. Wu, A. Sun, Y. Sun, and T. Sun, "Load Balancing and Remaining Visible Time based Handover Algorithm for LEO Satellite Network," in *Proc. IEEE International Conference on Computer and Communications (ICCC)*, 2022, pp. 391–395.

[12] Y. H. Lei, L. F. Cao, and M. Da Han, "A Handover Strategy Based on User Dynamic Preference for LEO Satellite," in *Proc. IEEE International Conference on Computer and Communications (ICCC)*, 2021, pp. 1925–1929.

[13] J. Li, K. Xue, J. Liu, and Y. Zhang, "A User-Centric Handover Scheme for Ultra-Dense LEO Satellite Networks," *IEEE Wireless Communications Letters*, vol. 9, no. 11, pp. 1904–1908, 2020.

[14] 3GPP, "Study on New Radio (NR) to Support Non-Terrestrial Networks," *v15.4.0*, 2020.

[15] ITU-R, "Attenuation by Atmospheric Gases and Related Effects," *P.676-13*, 2022.

[16] S. K. Sharma, S. Chatzinotas, and B. Ottersten, "Cognitive Beamhopping for Spectral Coexistence of Multibeam Satellites," in *Proc. IEEE Future Network & Mobile Summit*, 2013, pp. 1–10.

[17] L.-H. Shen, Y.-C. Chen, and K.-T. Feng, "Mobility-Aware Fast Beam Training Scheme for IEEE 802.11ad/ay Wireless Systems," in *Proc. IEEE Wireless Communications and Networking Conference (WCNC)*, 2018, pp. 1–6.

[18] L.-H. Shen, K.-T. Feng, and L. Hanzo, "Coordinated Multiple Access Point Multiuser Beamforming Training Protocol for Millimeter Wave WLANs," *IEEE Transactions on Vehicular Technology*, vol. 69, no. 11, pp. 13 875–13 889, 2020.

[19] L.-H. Shen, Y. Ho, K.-T. Feng, L.-L. Yang, S.-H. Wu, and J.-M. Wu, "Hierarchical Multi-Agent Multi-Armed Bandit for Resource Allocation in Multi-LEO Satellite Constellation Networks," in *Proc. IEEE Vehicular Technology Conference*, 2023, pp. 1–5.

[20] N. Levanon, "Quick Position Determination Using 1 or 2 LEO Satellites," *IEEE Transactions on Aerospace and Electronic Systems*, vol. 34, pp. 736 – 754, 1998.